Advances in Difference Equations
a SpringerOpen Journal

RESEARCH

Open Access

CrossMark

A Lycaon pictus impulsive state feedback control model with Allee effect and continuous time delay

Yaning Li[1], Huidong Cheng[1*] and Yanhui Wang[1,2]

*Correspondence:
chd900517@sdust.edu.cn
[1]College of Mathematics and
Systems Science, Shandong
University of Science and
Technology, Qingdao, China
Full list of author information is
available at the end of the article

Abstract

Allee effect (i.e. sparse effect) is active when the population density is small. Our purpose is to study such an effect of this phenomenon on population dynamics. We investigate an impulsive state feedback control single-population model with Allee effect and continuous delay. We first qualitatively analyze the singularity of this model. Then we obtain sufficient conditions for the existence of an order-one periodic orbit by the geometric theory of impulsive differential equations for the survival of endangered populations and obtain the uniqueness of an order-one periodic orbit by the monotonicity of the subsequent function. Furthermore, we prove the orbital asymptotic stability of an order-one periodic orbit using the geometric properties of successor functions to confirm the robustness of this control. Finally, we verify the correctness of our theoretical results by using some numerical simulations. Our results show that the release of artificial captive African wild dog (Lycaon pictus) can effectively protect the African wild dog population with Allee effect.

MSC: 34C25; 34D23; 92B05; 34A37

Keywords: Qualitatively analysis; Order-one periodic orbit; Impulsive differential equation; Allee effect

1 Introduction

The African wild dog is one of the endangered carnivorous species in South Africa. They are mainly distributed in parts of eastern and southern Africa. In the past few decades the habitat of African wild dog has been drastically reduced, and the population quantity has declined significantly [1]. Research suggests that there are many reasons for the sharp decline in the distribution and number of African wild dogs, which may include conflicts with humans, habitat loss, persecution and competition with other predators, genetic diversity of infectious diseases, and inbreeding depression [2]. The scholars analyzed the demographic data of endangered Lycaon pictus in Hluhluwe–Imfolozi Park in South Africa from 1980 to 2004. They found that the African wild dog population has an obvious Allee effect [3]. In 1931, W.C. Allee paid attention to the possibility of a positive relationship between individual aspects of fitness and population density [4]. In other words, when the species has a small population density, the death rate increases, and the birth rate decreases, then the risk of species extinction increases. There are many reasons

for this phenomenon. For example, for an individual, it is difficult to seek spouses and difficult to resist enemies and inbreeding depression [5]. Therefore many researches focus on the Allee effect (sparse effect) and have done a lot of work in this direction [6–9].

The Allee effect has been observed in many species, such as plants, marine invertebrates, and mammals [8]. For these species, there exists a minimum survival threshold, which implies that it is not necessary to adopt any measure to intervene when the population density is above this threshold [10]. But once the population density is lower than the survival threshold, some corresponding control measures should be performed according to the state of the target species. So the threshold strategy is also called the state feedback control strategy. This strategy can be precisely described by an impulsive differential equation in mathematics [11].

In recent years, impulsive differential equations have been used in various fields [12–20], such as disease control and pharmacology [21–29], integrated pest management [30–38], microbial culture [38–43], and protection of endangered animals and plants [44–51]. For example, Zhang et al. [10] focused on a predator–prey model with impulsive state feedback control and assuming that the spraying pesticide and releasing the natural enemies are taken at different thresholds. Liang et al. [5] investigated a state-dependent impulsive control model for computer virus propagation under media coverage, and the results show that the media coverage can delay the spread of computer virus. Nie et al. [52] studied different types of chemostat ecosystems of microbial cultures. However, there are few studies on the use of impulsive control strategies to protect the endangered species.

Assume that the model with Allee effect of African wild dog species is as follows:

$$\frac{dx}{dt} = x\left[r\left(1 - \frac{x}{K}\right) - \frac{a}{cax + 1}\right], \tag{1}$$

where K is the maximum capacity of the environment, r is the intrinsic growth rate, and $\frac{a}{cax+1}$ represents the Allee effect caused by mating restrictions. If $a > \sqrt{\frac{r}{ck}}$, then for system (1), there exists the Allee effect [8]. However, the population number of African wild dogs also depends on the population density at all times in the past. Therefore the investigation of continuous time delay in population dynamics has a great significance. Therefore we consider an African wild dog model with Allee effect and continuous time delay as follows:

$$\frac{dx}{dt} = x\left[r\left(1 - \frac{x}{K}\right) - \frac{a}{cax + 1} - \omega \int_{-\infty}^{t} e^{-b(t-s)}x(s)\, ds\right]. \tag{2}$$

We assume that $y(t) = \int_{-\infty}^{t} e^{-b(t-s)}x(s)\, ds$. We think that artificial breeding methods and monitoring the population size can protect the African wild dog. When the population number of African wild dogs reaches the minimum survival threshold h, the release of artificial captivity in the African wild dog population is considered as an effective method of protection. So we consider an African wild dog impulsive feedback control model with

Allee effect and continuous time delay as follows:

$$
\begin{cases}
\left.\begin{array}{l}
\frac{dx}{dt} = x[r(1 - \frac{x}{K}) - \frac{a}{cax+1} - \omega y], \\
\frac{dy}{dt} = x - by,
\end{array}\right\} \quad x > h, \\
\left.\begin{array}{l}
\triangle x(t) = p, \\
\triangle y(t) = 0,
\end{array}\right\} \quad\quad x = h.
\end{cases}
\tag{3}
$$

In this work, all the parameters are positive, and $\int_0^\infty e^{(-s)}\, ds = 1$.

The paper is organized is as follows. In Sect. 2, we first analyze qualitatively the singularity of system (3) without impulse effect by the Bendixson–Dulac theory. Then we use the geometric theory of impulsive differential equations to prove the existence of a periodic orbit. The uniqueness of the periodic orbit of model (3) is proved by the monotonicity of subsequent functions. Meanwhile, the geometric properties of subsequent functions are used to prove the stability of the periodic orbit of system (3) in Sect. 3. In Sect. 4, we illustrate the correctness of the results obtained by some numerical simulations. Finally, we conclude our work.

2 Dynamic analysis of system (3)

2.1 Qualitative analysis of system (3)

In this subsection, we first discuss system (3) without impulse. Thus we consider the following system:

$$
\begin{cases}
x'(t) = x(t)[r(1 - \frac{x(t)}{K}) - \frac{a}{cax(t)+1} - \omega y(t)] \triangleq P(x, y), \\
y'(t) = x(t) - by(t) \triangleq Q(x, y).
\end{cases}
\tag{4}
$$

Then, we solve the system

$$
\begin{cases}
x(t)[r(1 - \frac{x(t)}{K}) - \frac{a}{cax(t)+1} - \omega y(t)] = 0, \\
x(t) - by(t) = 0.
\end{cases}
\tag{5}
$$

Obviously, system (3) has the equilibrium point $O(0, 0)$ and a positive equilibrium point $E^*(x^*, y^*)$, where

$$
x^* = \frac{(rcabK - rb - \omega K) + \sqrt{\Delta}}{2(rcab + \omega caK)},
$$

$$
y^* = \frac{(rcabK - rb - \omega K) + \sqrt{\Delta}}{2b(rcab + \omega caK)},
$$

and

$$
\Delta = (rcabK - rb - \omega K)^2 + 4(rK - aK)(rcab^2 + \omega Kca).
$$

Let

$$
(H_1) : K < 2x^*
$$

and

$$(H_2): \sqrt{\frac{r}{cK}} < a < 2b.$$

Theorem 2.1 *If (H_1) holds, then the point $E^*(x^*, y^*)$ is locally asymptotically stable.*

Proof The Jacobian matrix at the point $E^*(x^*, y^*)$ is

$$J = \begin{pmatrix} r - \dfrac{2rx^*}{K} - \dfrac{a}{(cax^* + 1)^2} - \omega y^* & -\omega \\ 1 & -b \end{pmatrix}.$$

Iif (H_1) holds, then we have

$$\mathrm{tr}\big(J\big(E^*\big)\big) = r - \frac{2rx^*}{K} - \frac{a}{(cax^* + 1)^2} - \omega y - b < 0$$

and

$$\mathrm{Det}\big(J\big(E^*\big)\big) = -b\left[r - \frac{2rx^*}{K} - \frac{a}{(cax^* + 1)^2} - \omega y \right] + \omega > 0.$$

Thus the point $E^*(x^*, y^*)$ is a locally asymptotically stable node or focus. □

Theorem 2.2 *If (H_1) and (H_2) hold, then the point $E^*(x^*, y^*)$ is globally asymptotically stable.*

Proof Let $B = \frac{1}{x}$. Then

$$\begin{aligned} D &= \frac{\partial(PB)}{\partial x} + \frac{\partial(QB)}{\partial y} \\ &= -\frac{r}{K} + \frac{ca^2}{(cax + 1)^2} - \frac{b}{x} \\ &= \frac{Kca^2 x - r(cax + 1)^2 - bK(cax + 1)^2}{(cax + 1)^2} \\ &= \frac{-rc^2 a^2 x^3 - 2carx^2 - rx - bKc^2 a^2 x^2 - 2cabKx - bK + cKa^2 x}{(cax + 1)^2} \\ &= \frac{caKx(a - 2b) - rc^2 a^2 x^3 - 2carx^2 - rx - bKc^2 a^2 x^2 - bK}{(cax + 1)^2}. \end{aligned}$$

Obviously, if (H_2) holds, then the function

$$D = \frac{\partial(PB)}{\partial x} + \frac{\partial(QB)}{\partial y} < 0.$$

In other words, system (4) has no limit cycle in $R_2^+ = \{(x, y) | x \geq 0, y \geq 0\}$, and every solution of system (4) is bounded in R_2^+. According to the method in [8], the point $E^*(x^*, y^*)$ is a globally asymptotically stable focus or node (see Fig. 1). □

Figure 1 Phase diagram of system (3) with $r = 1$, $K = 5, b = 2, a = 0.5, \omega = 0.1, c = 3$
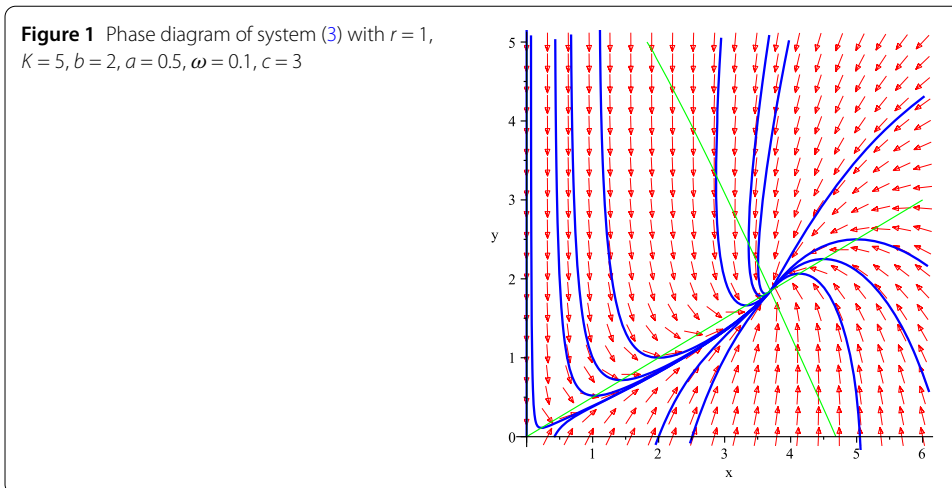
2.2 Dynamic analysis of an order-one periodic orbit of system (3)

2.2.1 *System (3) has a unique periodic orbit*

In this subsection, we study the existence and uniqueness of an order-one periodic orbit. We assume that the impulsive set $M = \{(x,y) \in R_2^+ | x = h, y \geq 0\}$ and phase set $N = \{(x,y) \in R_2^+ | x = h + p, y \geq 0\}$ are straight lines. The trajectory that starts from any point A is denoted by $f(A,t)$. A positive equilibrium $E^*(x^*, y^*)$ is globally asymptotically stable if conditions (H_1) and (H_2) hold.

Theorem 2.3

(1) *If $0 < h < h + p \leq x^*$, then system (3) has no order-one periodic orbit.*

(2) *If $0 < h < x^* < h + p < K$, then system (3) has no order-one periodic orbit.*

Proof Case 1. $0 < h < h + p \leq x^*$.

If $0 < h < h + p \leq x^*$, then the impulsive set M and the phase set N are on the left of the point $E^*(x^*, y^*)$. The impulsive set M and the phase set N intersect the x-axis at the points $M'(h, 0)$ and $N'(h + p, 0)$, respectively. The isoclinic line $\dot{x} = 0$ intersects with the x-axis at the point $E'(\tau, 0)$, where

$$\tau = \frac{(rKca - r) + \sqrt{\Theta}}{2rca}$$

and

$$\Theta = (rKca - r)^2 + 4rca(rK - aK).$$

The intersection point of the isoclinic line $\dot{x} = 0$ and the impulsive set M is $F_1(h, y_{F_1})$, where

$$y_{F_1} = \frac{(ahc + 1)(rK - rh) - aK}{\omega K(ahc + 1)}.$$

According to the biological background, we only have to study the dynamic behavior of such a system in the region $\Phi = \{(x,y) | x \geq h, 0 < y \leq b_M - Kx\}$, where b_M is a sufficiently large constant satisfying $\frac{d\chi}{dt}|_{\chi=0} < 0$.

Let

$$\chi : Kx + y - b_M = 0.$$

Then we have

$$\frac{d\chi}{dt}\Big|_{\chi=0} = \frac{Kdx}{dt} + \frac{dy}{dt}$$

$$= x - b_M y + K\left[x\left(r - \frac{rx}{K}\right) - \frac{a}{cax+1} - \omega y\right]$$

$$= x + rKx - rx^2 - \frac{aK}{cax+1} - \omega Ky - b_M y$$

$$= (1 + rK)x - rx^2 - \frac{aK}{cax+1} - (\omega K + b_M)y < 0.$$

This implies that there must exist an intersection point of the trajectory $f(F_1, t)$ and the phase set N denoted by $F(h + p, y_F)$. The point F_1 jumps to the point F^1 due to the impulse effect. According to the definition of the subsequent function in [5] and the trajectory tend of system (3), the subsequent function of the point F is

$$g(F) = y_{F^1} - y_F < 0.$$

The trajectory $f(N', t)$ will have no intersection point with the impulsive set M. Thus, the trajectory starting from any point located on the segment $\overline{FN'} \subset N$ is attractive to the positive equilibrium point E^* by impulse effect. The orbit starting from any point that is above the point F is also attractive to the point E^* by several impulsive effects at most.

In summary, system (3) has no order-one periodic orbit when $0 < h < h + p \leq x^*$ (see Fig. 2).

Case 2. $0 < h < x^* < h + p < K$

If $0 < h < x^* < h + p < K$ holds, then the point $E^*(x^*, y^*)$ is between the impulsive set M and the phase set N. The isoclinic line $\dot{x} = 0$ intersects the impulsive set M at the point

Figure 2 Existence of order-one periodic orbit if $0 < h < h + p \leq x^*$
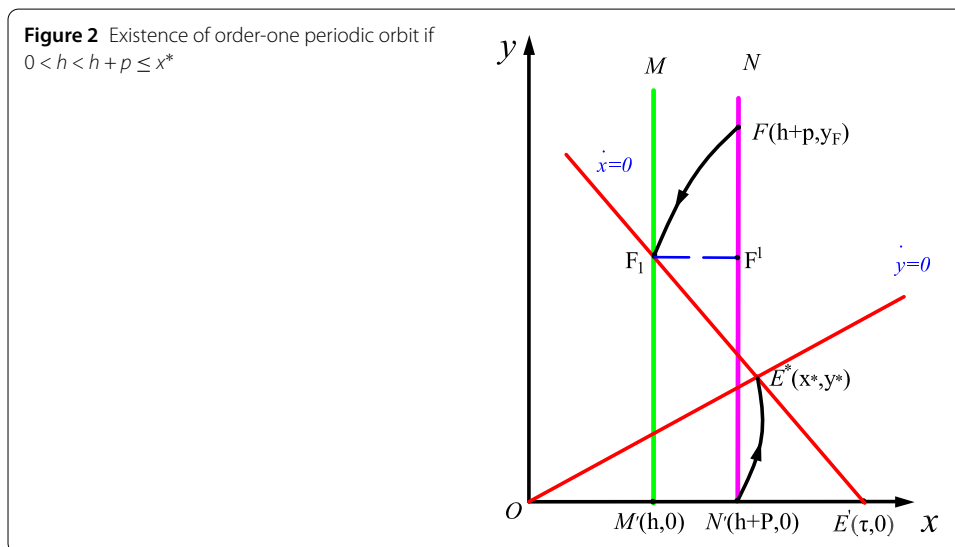
$F_1(h, y_{F_1})$. The impulsive set M intersects the x-axis at the point $M'(h, 0)$, and the intersection point of the phase set N and the x-axis is the point $N'(h + p, 0)$.

Thus the orbit $f(N', t)$ tends to the point $E^*(x^*, y^*)$, and the trajectory $f(F_1, t)$ surely has an intersection point with the phase set N, denoted by $F(h + p, y_F)$, where

$$y_F > y^* = \frac{(rcabK - rb - \omega K) + \sqrt{\Delta}}{2b(rcab + \omega caK)}.$$

Thus the point F_1 will jump to the point $F^1 \in N$ by the impulse effect. So the subsequent function of the point F is

$$g(F) = y_{F^1} - y_F < 0.$$

Similarly, the orbit that starts from any point on the segment $\overline{FN'} \subset N$ will tend to the positive equilibrium point $E^*(x^*, y^*)$, and the trajectory starting from any point above the point F on the phase set N will also be attractive to the point E^* by several impulse effects at most.

Thus, system (3) has no order-one periodic orbit if $0 < h < x^* < h + p < K$ (see Fig. 3). □

Theorem 2.4 *If* $0 < x^* \leq h < h + p < K$, *then system* (3) *has an order-one periodic orbit, and when* $h + p > \frac{\sqrt{\Lambda} + (brkca - \omega r - br)}{2(brca + \omega Kca)}$, *the order-one periodic orbit is unique.*

Proof Let $0 < x^* \leq h < h + p < K$. Then the positive equilibrium point E^* is on the left of the impulsive set M. The phase set N intersects the isoclinic line $\dot{x} = 0$ and $\dot{y} = 0$ at the points $P(h + p, y_P)$ and $H(h + p, \frac{h+p}{b})$, respectively, where

$$y_P = \frac{-rca(h + p)^2 + (rKca - r)(h + p) + K(r - a)}{\omega Kca(h + p) + \omega K}.$$

By the asymptotic stability of the point E^* the trajectory $f(H, t)$ intersects the impulsive set M at the point H_1, then it hits the impulsive set M at the point $H^1(h + p, y_{H^1})$ on the

Figure 3 Existence of order-one periodic orbit if $0 < h < x^* < h + p < K$
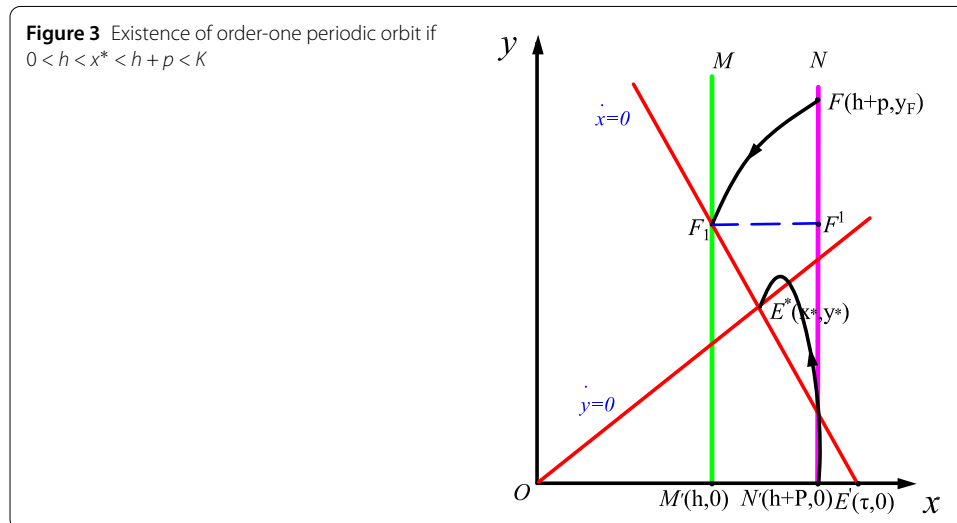
phase set N. The successor point H^1 of the point H is surely under the point H, so $y_{H^1} < y_H$. Then the subsequent function of the point H is

$$g(H) = y_{H^1} - y_H < 0.$$

The trajectory $f(P,t)$ hits the impulsive set M at the point P_1, then jumps to the point $P^1(h+p, y_{P^1})$ by the impulsive effect. The successor point P^1 of the point P must be above the point P by the trajectory tend of system (3). Thus the subsequent function of the point P is

$$g(P) = y_{P^1} - y_P > 0.$$

By [10] there must be a point S between the points H and F such that

$$g(S) = 0,$$

and thus the orbit $f(S,t)$ is an order-one periodic orbit of system (3) when $0 < x^* < h < h + p < K$ (see Fig. 4).

Now, we prove the uniqueness of the order-one periodic orbit of system (3).

We choose any two points $G(h+p, y_G)$ and $I(h+p, y_I)$ such that

$$y_G > y_I.$$

The intersection point of the trajectory $f(G,t)$ and the impulsive set M is the point G_1. Then the point G_1 jumps to the point G^1 by impulse effects. The subsequent function of the point G is

$$g(G) = y_{G^1} - y_G.$$

The intersection point of the orbit $f(I,t)$ and the impulsive set M is the point I_1,.Then the point I_1 jumps to the point I^1 by impulse effects. The subsequent function of the point

Figure 4 Existence and uniqueness of order-one periodic orbit if $0 < x^* \le h < h + p < K$
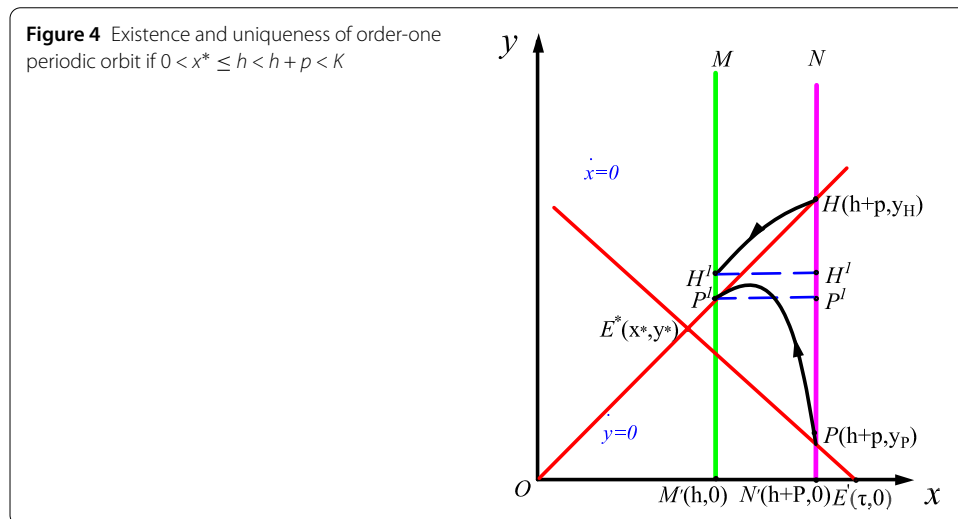
I is

$$g(I) = y_{I^1} - y_I.$$

Let the function $y_{(x,Q_0)}$ be denoted by the coordinates of an arbitrary point on the trajectory $f(Q_0, t)$, where Q_0 is the starting point. According to

$$y_G > y_I,$$

we define

$$y_G(x) \triangleq y_{(x,G)}, \qquad y_I(x) \triangleq y_{(x,I)}$$

and

$$d_{GI} = y_G(x) - y_I(x), \quad x \in [h, h + p].$$

Hence we have

$$d'_{GI}(x) = y'_G(x) - y'_I(x)$$

$$= \frac{K(cax + 1)}{x} \left[\frac{x - by_G}{(rK - rx - \omega y_G K)(cax + 1) - aK} \right.$$

$$\left. - \frac{x - by_I}{(rK - rx - \omega y_I K)(cax + 1) - aK} \right]$$

$$= \frac{K(cax + 1)}{x} \phi'(\varsigma)(y_G - y_I),$$

where

$$\phi(y) = \frac{x - by}{(rK - rx - \omega yK)(cax + 1) - aK}$$

and

$$\phi'(y) = \frac{-b[(cax + 1)(rK - rx - \omega Ky)] + \omega K(cax + 1)(x - by)}{[(cax + 1)(rK - rx - \omega Ky) - aK]^2}$$

$$= \frac{-brcaKx + brcax^2 - brK + brx + \omega Kcax^2 + \omega Kx}{[(cax + 1)(rK - rx - \omega Ky) - aK]^2}$$

$$= \frac{(brca + \omega Kca)x^2 + (\omega K + br - brkca)x - brk}{[(cax + 1)(rK - rx - \omega Ky) - aK]^2}$$

when

$$h + p > \frac{\sqrt{\Lambda} + (brkca - \omega r - br)}{2(brca + \omega Kca)},$$

where

$$\Lambda = (\omega K + br - brKca)^2 + 4brK(brKa + \omega Kca).$$

Then

$$\phi'(y) > 0,$$

and thus

$$d'_{GI} > 0$$

for $x \in [h, h + p]$. In summary, the function $d_{GI}(x)$ is an increasing function, and

$$d_{GI}(h + p) > d_{GI}(h).$$

Let

$$d_1 = d_{GI}(h + p) = y_G - y_I,$$
$$d_2 = d_{GI}(h) = y_{G^1} - y_{I^1}.$$

Obviously,

$$d_1 > d_2.$$

Hence the subsequent function of the points G and I satisfies

$$
\begin{aligned}
g(G) - g(I) &= (y_{G^1} - y_G) - y_{I^1} = y_I \\
&= -(y_G - y_I) + (y_{G^1} - y_{I^1}) \\
&= d_2 - d_1 < 0.
\end{aligned}
$$

Thus, the successor function is decreasing monotonously on the phase set N. So there must exist a unique point S such that $g(S) = 0$. This means that the order-one periodic orbit of system (3) is unique. □

3 Stability of the order-one periodic solution

Theorem 3.1 *The periodic orbit of system* (3) *is orbitally asymptotically stable.*

Proof By Theorems 2.3 and 2.4 system (3) has a unique order-one periodic orbit between the points H and F, and $y_F < y_S < y_H$. Thus $g(F) > 0$ for any $F \in N$ with $y_S > y_F$, $g(H) < 0$ for any $H \in N$ with $y_H > y_S$, and $g(F) = g(H) = 0$ if and only if $H = F = S$.

Then we choose an arbitrary point F^0 on the phase set N. If $F^0 \in N/\overline{FS}$, then after several impulse effects, the orbit jumps to the segment $\overline{FS}$. Hence we assume that $F^0 \in \overline{FS} \subset N$. The orbit $f(F^0, t)$ hits the impulsive set M at the point F_1, then the point F_1 jumps to the point $F^1 \in N$ after an impulse effect, and

$$y_F < y_{F^0} < y_{F_1} = y_{F^1} < y_S.$$

The orbit $f(F^1, t)$ intersects the impulsive set M at the point F_2, then jumps to the point $F^2 \in N$, and

$$y_F < y_{F^0} < y_{F^1} < y_{F^2} < y_S.$$

The orbit $f(F^2, t)$ hits the impulsive set M at the point F_3, then jumps to the point $F^3 \in N$, and

$$y_F < y_{F^0} < y_{F^1} < y_{F^2} < y_{F^3} < y_S.$$

Repeating this process, we get a point sequence $\{F^k\}$, where $k = 0, 1, 2, \ldots$, such that

$$y_F < y_{F^0} < y_{F^1} < \cdots < y_{F^k} < \cdots \leq y_S.$$

Then the sequence $F^k \|_{k=0,1,2,\dots}$ is an increasing sequence with upper bound y_S. According to the monotone bounded theorem, there exists the limit $\lim_{k\to\infty} y_{F^k} = y_{S'}$, which implies that

$$g(S') = g\left(\lim_{k\to\infty} y_{F^k}\right) = \lim_{k\to\infty} g(y_{F^k}) = \lim_{k\to\infty}(y_{F^{k+1}} - y_{F^k}) = 0.$$

Since $g(F) = 0$ if and only if $F = S$, we get $S' = S$, that is,

$$\lim_{k\to\infty} g(y_{F^K}) = y_{S'} = y_S.$$

Similarly, by the same method we obtain a point sequences $I^k \|_{k=0,1,2,\dots}$ such that

$$y_S \leq \cdots < y_{I^k} < \cdots < y_{I^2} < y_{I^1} < y_{I^0} < y_I.$$

Since $\{I^k\}$ is an decreasing sequence with lower bound y_S, by the monotone bounded theorem it has the limit $\lim_{k\to\infty} y_{I^k} = y_{S'}$, which means that

$$g(S') = g\left(\lim_{k\to\infty} y_{I^k}\right) = \lim_{k\to\infty} g(y_{I^K}) = \lim_{k\to\infty}(y_{I^{k+1}} - y_{I^k}) = 0.$$

Since $g(I) = 0$ if and only if $I = S$, we get $S' = S$, that is, $y_{I^k} = y_S$. Then we have

$$y_F < y_{F^0} < y_{F^1} < \cdots < y_{F^k} < \cdots \leq y_S \leq \cdots < y_{I^k} < \cdots < y_{I^2} < y_{I^1} < y_{I^0} < y_I.$$

By the arbitrariness of the points I^0 and F^0 we have

$$\lim_{k\to\infty} y_{I^k} = \lim_{k\to\infty} y_{F^k} = y_S.$$

In summary, all orbits of system (3) tend to the order-one periodic orbit (see [5]). So the order-one periodic orbit of system (3) is orbitally asymptotically stable and globally attractive (see Fig. 5). □

Figure 5 Orbital asymptotically stability of the order-one periodic orbit of system (1)
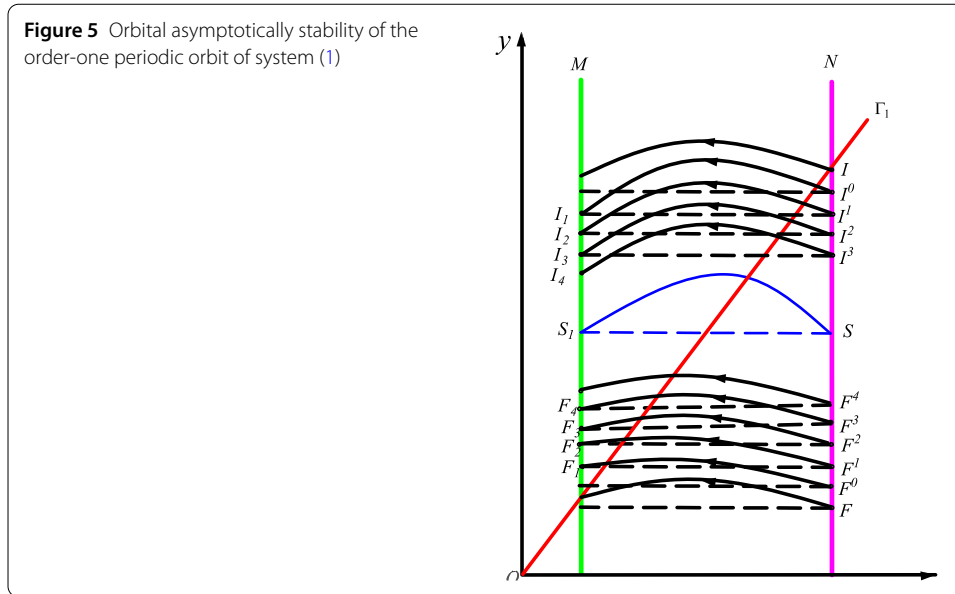
Thus our theoretical results show that releasing the African wild dogs in captivity to the wild is effective for protecting African wild dog population with Allee effect and continuous delay. Therefore, when protecting African wild dogs, we can determine the survival threshold, have African wild dogs in captivity, and monitor the wild populations (the initial value). Then, according to the state feedback of wild white-headed langurs, a certain amount of white-headed langurs in captivity will be released to the wild to increase the number of white-headed langurs in the wild, making the population have a normal reproduction to survive. According to the survival threshold and initial value, we can choose different grazing plans.

4 Numerical simulations and conclusion

4.1 Numerical simulations

In this section, we verify the correctness of the results by two examples.

Example 4.1 Let $r = 1$, $K = 5$, $\omega = 0.1$, $b = 2$, $c = 3$, and $a = 0.5$. By calculations we obtain the point $E^*(3.694254177, 10847127088)$. Thus system (3) becomes

$$
\begin{cases}
\frac{dx}{dt} = x[1(1 - \frac{x}{5}) - \frac{0.5}{1.5x+1} - 0.1y], \\
\frac{dy}{dt} = x - 2y,
\end{cases} \quad x > h, \\
\begin{cases}
\triangle x(t) = 0.8, \\
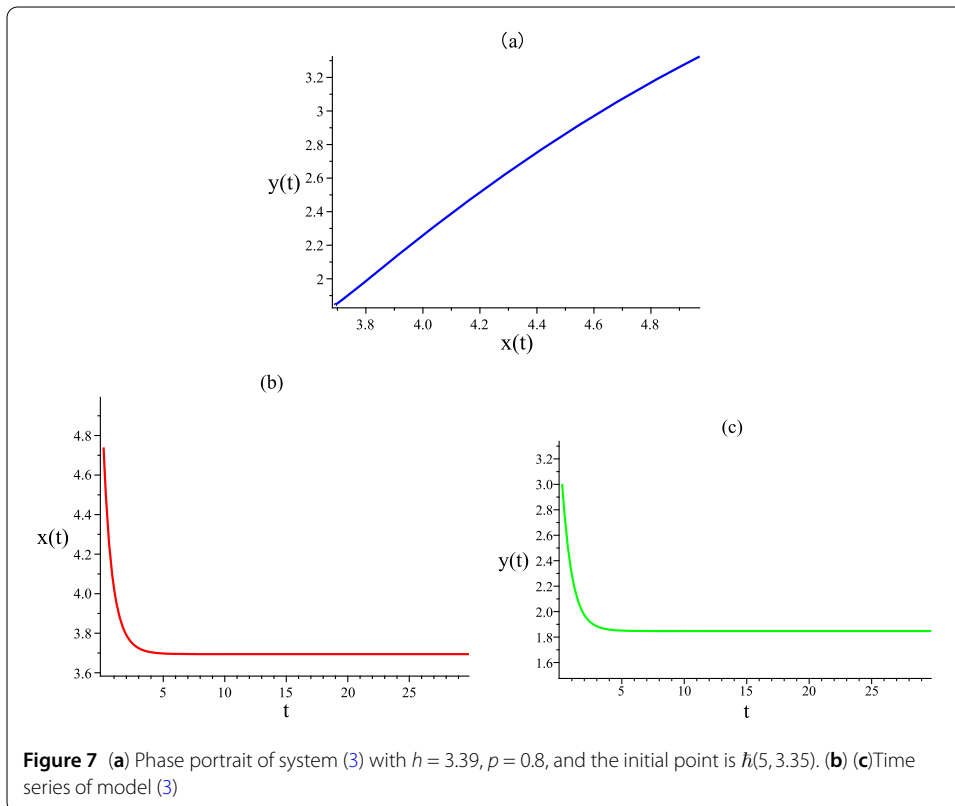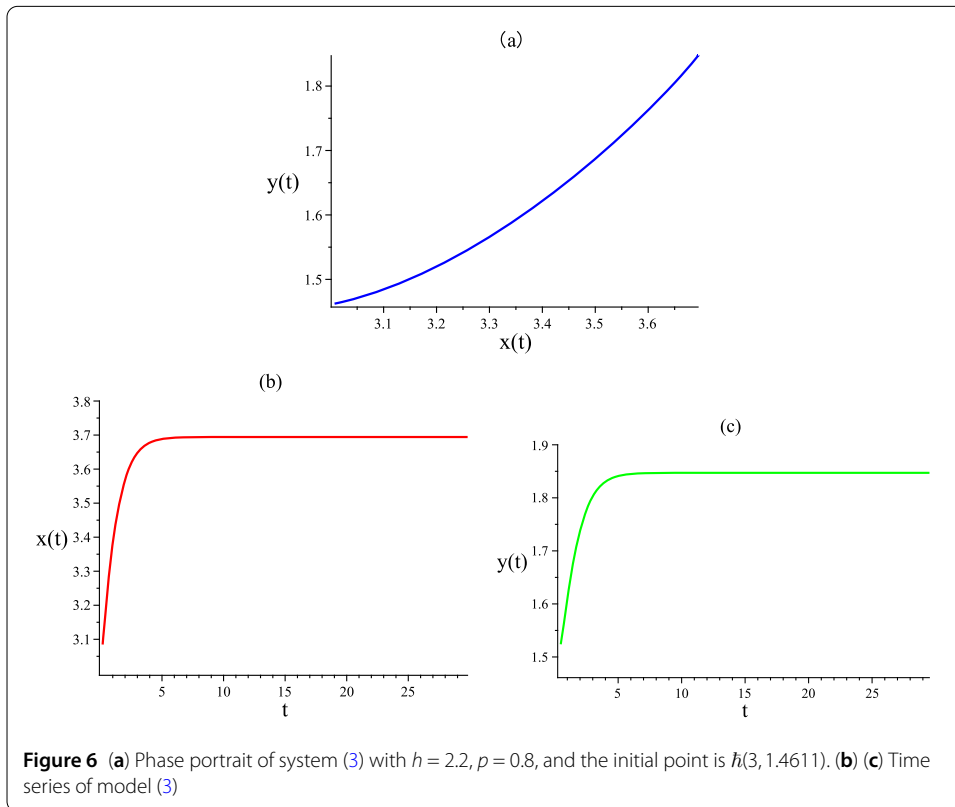\triangle y(t) = 0,
\end{cases} \quad x = h.
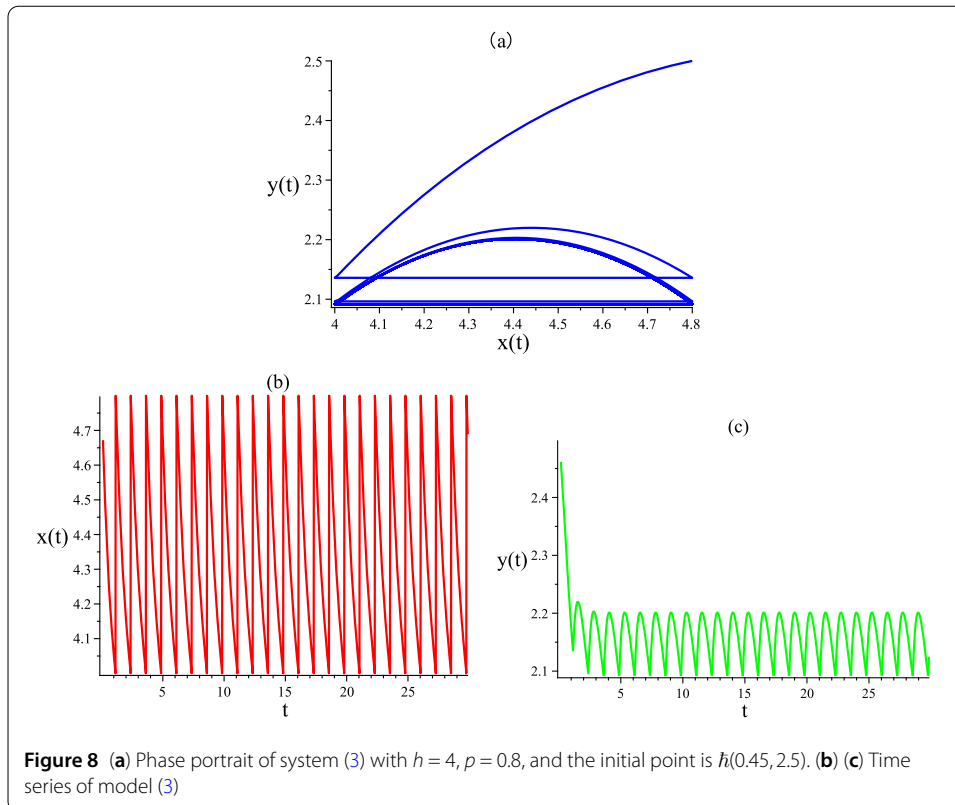$$
(6)

Then we get the following cases.

Case I: Let $h = 2.2$, $p = 0.8$. Then $0 < h < h + p < x^*$. See Fig. 6.

Case II: Let $h = 3.39$, $p = 0.8$. Then $0 < h < x^* < h + p < K$. See Fig. 7.

Case III: Let $h = 4$, $p = 0.8$. Then $0 < x^* < h < h + p < K$. See Fig. 8.

Example 4.2 We verify the feasibility of feedback control strategy by a real-life example.

Figure 6 (**a**) Phase portrait of system (3) with $h = 2.2$, $p = 0.8$, and the initial point is $\hbar(3, 1.4611)$. (**b**) (**c**) Time series of model (3)

Figure 7 (**a**) Phase portrait of system (3) with $h = 3.39$, $p = 0.8$, and the initial point is $\hbar(5, 3.35)$. (**b**) (**c**)Time series of model (3)

Figure 8 (**a**) Phase portrait of system (3) with $h = 4$, $p = 0.8$, and the initial point is $\hbar(0.45, 2.5)$. (**b**) (**c**) Time series of model (3)
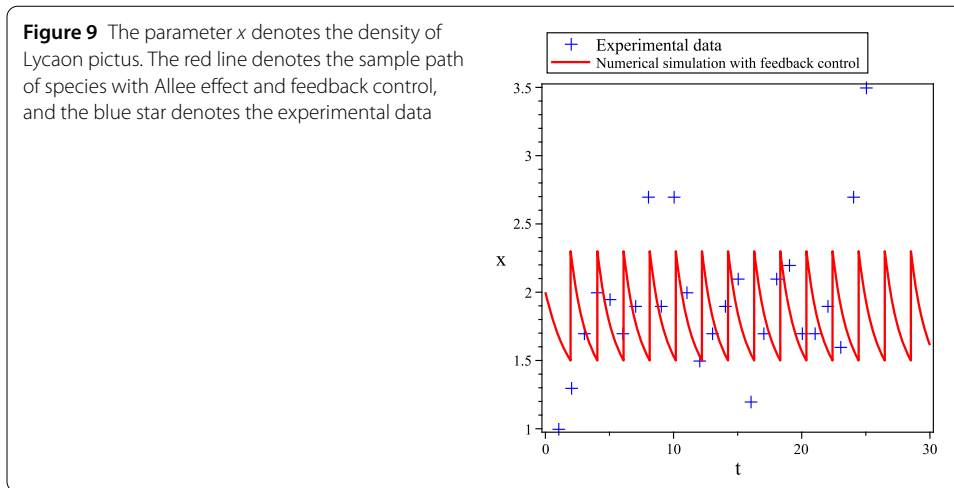
In [8], the authors studied the data from 1980–2004 on a small region population of Lycaon pictus in Hluhluwe–Imfolozi Park (HIP) to analyze the pack and population density dynamics. According to these data in [8], the authors take the annual growth rate of Lycaon pictus is 0–1.47, the carrying capacity K is 2.2–13.3, the parameter a is 0.6–1.3, and c is 0.5–1.2. Thus, we assume that the initial value of the pack is 2. We determine the minimum survival threshold by monitoring the population of Lycaon pictus in the wild; when the population of Lycaon pictus decreases to 1.5, a certain amount of Lycaon pictus in captivity is released to the wild. Let the parameters $r = 1$, $K = 2.5$, $a = 0.7$, $c = 1$, $\omega = 0.1$, and $b = 1$ (see Fig. 9). Numerical simulation shows that the feedback control strategy can effectively protect the Lycaon pictus population.

4.2 Conclusion

In this paper, we studied the African wild dogs impulsive state feedback control model with Allee effect and continuous time delay. By the feedback information of the density of African wild dog population from the monitor we can protect the African wild dog population.

First, we carried on the quantitative and qualitative analysis and obtained two conditions (H_1) and (H_2). We proved the global asymptotic stability of the positive equilibrium $E^*(x^*, y^*)$ by the Bendixson–Dulac theory.

Then we proved that the existence of an order-one periodic orbit of system (3) by the geometric theory of differential equations. We also proved the uniqueness of the order-one periodic orbit of system (3) by the monotonicity of the successor functions and the Lagrange mean value theorem.

Figure 9 The parameter *x* denotes the density of Lycaon pictus. The red line denotes the sample path of species with Allee effect and feedback control, and the blue star denotes the experimental data

Finally, we studied the orbital asymptotic stability of the order-one periodic orbit by the geometric properties of successor functions. Then we proved that the limit exists by the uniqueness of the order-one periodic orbit and the limit existence theorem.

All the results suggest that the release of artificial captive of African wild dogs can effectively protect the African wild dog population with Allee effect. The determination of the value of the survival threshold h involves analyzing the viability of the African wild dog population, which will be our future work.

Author details
[1]College of Mathematics and Systems Science, Shandong University of Science and Technology, Qingdao, China. [2]State Key Laboratory of Mining Disaster Prevention and Control Co-founded by Shandong Province and the Ministry of Science and Technology, Shandong University of Science and Technology, Qingdao, China.

Publisher's Note
Springer Nature remains neutral with regard to jurisdictional claims in published maps and institutional affiliations.

References
1. Lindsey, P.A., Alexander, R.R., Toit, J.T.D., Mills, M.G.L.: The potential contribution of ecotourism to African wild dog Lycaon pictus conservation in South Africa. Biol. Conserv. **123**(3), 339–348 (2005)
2. Courchamp, F., Brock, T.C., Grenfell, B.: Multipack dynamics and the Allee effect in the African wild dog, *lycaon pictus*. Anim. Conserv. **3**(4), 277–285 (2000)
3. Somers, M.J., Graf, J.A., Szykman, M., Slotow, R., Gusset, M.: Dynamics of a small re-introduced population of wild dogs over 25 years: Allee effects and the implications of sociality for endangered species' recovery. Oecologia **158**(2), 239 (2008)
4. Stephens, P.A., Sutherland, W.J., Freckleton, R.P.: What is the Allee effect? Oikos **87**(1), 185–190 (1999)
5. Chen, S., Xu, W., Chen, L., Huang, Z.: A white-headed langurs impulsive state feedback control model with sparse effect and continuous delay. Commun. Nonlinear Sci. Numer. Simul. **50**, 88–102 (2017)
6. Chen, L.: Pest control and geometric theory of semi-continuous dynamical system. J. Beihua Univ. Nat. Sci. **12**(1), 1–12 (2011)

7. Liu, Q., Huang, L., Chen, L.: A pest management model with state feedback control. Adv. Differ. Equ. **2016**(1), 292 (2016)

8. Yu, X., Yuan, S., Zhang, T.: Persistence and ergodicity of a stochastic single species model with Allee effect under regime switching. Commun. Nonlinear Sci. Numer. Simul. **59**, 359–374 (2018)

9. Bian, F., Zhao, W., Song, Y., Yue, R.: Dynamical analysis of a class of prey–predator model with Beddington–DeAngelis functional response, stochastic perturbation, and impulsive toxicant input. Complexity **2017**, Article ID 3742197 (2017). https://doi.org/10.1155/2017/3742197

10. Zhang, T., Ma, W., Meng, X., Zhang, T.: Periodic solution of a prey–predator model with nonlinear state feedback control. Appl. Math. Comput. **266**, 95–107 (2015)

11. Liang, Z., Zeng, X., Pang, G., Liang, Y.: Periodic solution of a Leslie predator-prey system with ratio-dependent and state impulsive feedback control. Nonlinear Dyn. **89**(4), 2941–2955 (2017). https://doi.org/10.1007/s11071-017-3637-4

12. Li, Y., Cheng, H., Wang, J., Wang, Y.: Dynamic analysis of unilateral diffusion Gompertz model with impulsive control strategy. Adv. Differ. Equ. **2018**(1), 32 (2018)

13. Wang, J., Cheng, H., Li, Y., Zhang, X.: The geometrical analysis of a predator–prey model with multi-state dependent impulsive. J. Appl. Anal. Comput. **8**(2), 427–442 (2018)

14. Cheng, H., Zhang, T., Wang, F.: Existence and attractiveness of order one periodic solution of a Holling I predator–prey model. Abstr. Appl. Anal. **2012**, Article ID 126018 (2012). https://doi.org/10.1155/2012/126018

15. Liu, F.: Continuity and approximate differentiability of multisublinear fractional maximal functions. Math. Inequal. Appl. **21**(1), 25–40 (2018)

16. Liu, B., Tian, Y., Kang, B.: Existence and attractiveness of order one periodic solution of a Holling II predator–prey model with state-dependent impulsive control. Int. J. Biomath. **5**(03), 675 (2012)

17. Huang, M., Song, X., Li, J.: Modelling and analysis of impulsive releases of sterile mosquitoes. J. Biol. Dyn. **11**(1), 147 (2017)

18. Zhang, S., Meng, X., Wang, X.: Application of stochastic inequalities to global analysis of a nonlinear stochastic SIRS epidemic model with saturated treatment function. Adv. Differ. Equ. **2018**(1), 50 (2018)

19. Liu, F., Xue, Q., Yabuta, K.: Rough maximal singular integral and maximal operators supported by subvarieties on Triebel–Lizorkin spaces. Nonlinear Anal. **171**, 41–72 (2018)

20. Braverman, E., Liz, E.: Global stabilization of periodic orbits using a proportional feedback control with pulses. Nonlinear Dyn. **67**(4), 2467–2475 (2012)

21. Zhang, M., Song, G., Chen, L.: A state feedback impulse model for computer worm control. Nonlinear Dyn. **85**(3), 1561–1569 (2016)

22. Zhang, T., Meng, X., Song, Y., Zhang, T.: A stage-structured predator–prey SI model with disease in the prey and impulsive effects. Math. Model. Anal. **18**(4), 505–528 (2013)

23. Meng, X., Zhao, S., Feng, T., Zhang, T.: Dynamics of a novel nonlinear stochastic SIS epidemic model with double epidemic hypothesis. J. Math. Anal. Appl. **433**(1), 227–242 (2016)

24. Miao, A., Wang, X., Zhang, T., Wang, W., Sampath Aruna Pradeep, B.: Dynamical analysis of a stochastic SIS epidemic model with nonlinear incidence rate and double epidemic hypothesis. Adv. Differ. Equ. **2017**(1), 226 (2017)

25. Guo, H., Chen, L., Song, X.: Dynamical properties of a kind of SIR model with constant vaccination rate and impulsive state feedback control. Int. J. Biomath. **10**(7), 1750093 (2017). https://doi.org/10.1142/S1793524517500930

26. Wang, W., Zhang, T.: Caspase-1-mediated pyroptosis of the predominance for driving CD4$^+$ T cells death: a nonlocal spatial mathematical model. Bull. Math. Biol. **80**(3), 540–582 (2018)

27. Leng, X., Feng, T., Meng, X.: Stochastic inequalities and applications to dynamics analysis of a novel SIVS epidemic model with jumps. J. Inequal. Appl. **2017**(1), 138 (2017)

28. Miao, A., Jian, Z., Zhang, T., Pradeep, B.G.S.A.: Threshold dynamics of a stochastic SIR model with vertical transmission and vaccination. Comput. Math. Methods Med. **2017**, Article ID 4820183 (2017). https://doi.org/10.1155/2017/4820183

29. Li, F., Meng, X., Wang, X.: Analysis and numerical simulations of a stochastic SEIQR epidemic system with quarantine-adjusted incidence and imperfect vaccination. Comput. Math. Methods Med. **2018**(2), 1–14 (2018)

30. Cheng, H., Zhang, T.: A new predator–prey model with a profitless delay of digestion and impulsive perturbation on the prey. Appl. Math. Comput. **217**(22), 9198–9208 (2011)

31. Wang, J., Cheng, H., Meng, X., Pradeep, B.S.A.: Geometrical analysis and control optimization of a predator–prey model with multi state-dependent impulse. Adv. Differ. Equ. **2017**(1), 252 (2017)

32. Wang, J., Cheng, H., Liu, H., Wang, Y.: Periodic solution and control optimization of a prey–predator model with two types of harvesting. Adv. Differ. Equ. **2018**(1), 41 (2018)

33. Liu, H., Cheng, H.: Dynamic analysis of a prey-predator model with state-dependent control strategy and square root response function. Adv. Differ. Equ. **2018**(1), 63 (2018). https://doi.org/10.1186/s13662-018-1507-0

34. Zhang, H., Chen, L., Georgescu, P.: Impulsive control strategies for pest management. J. Biol. Syst. **15**(02), 235–260 (2007)

35. Zhang, H., Jiao, J., Chen, L.: Pest management through continuous and impulsive control strategies. Biosystems **90**(2), 350–361 (2007)

36. Jiang, G., Lu, Q.: Impulsive state feedback control of a predator-prey model. J. Comput. Appl. Math. **200**(1), 193–207 (2007)

37. Liu, X., Zhang, T., Meng, X., Zhang, T.: Turing-Hopf bifurcations in a predator-prey model with herd behavior, quadratic mortality and prey-taxis. Phys. A, Stat. Mech. Appl. **496**, 446–460 (2018)

38. Lv, X., Wang, L., Meng, X.: Global analysis of a new nonlinear stochastic differential competition system with impulsive effect. Adv. Differ. Equ. **2017**(1), 296 (2017)

39. Zhang, T., Ma, W., Meng, X.: Global dynamics of a delayed chemostat model with harvest by impulsive flocculant input. Adv. Differ. Equ. **2017**, 115 (2017)

40. Meng, X., Wang, L., Zhang, T.: Global dynamics analysis of a nonlinear impulsive stochastic chemostat system in a polluted environment. J. Appl. Anal. Comput. **6**(3), 865–875 (2016)

41. Zhang, T., Zhang, T., Meng, X.: Stability analysis of a chemostat model with maintenance energy. Appl. Math. Lett. **68**, 1–7 (2017)

42. Chi, M., Zhao, W.: Dynamical analysis of multi-nutrient and single microorganism chemostat model in a polluted environment. Adv. Differ. Equ. **2018**(1), 120 (2018)
43. Jiao, J., Cai, S., Liu, W., Li, L.: Dynamics of a competitive population system with impulsive reduction of the invasive population. Electron. J. Differ. Equ. **2017**, Article ID 281 (2017)
44. Zhang, T., Liu, X., Meng, X., Zhang, T.: Spatio-temporal dynamics near the steady state of a planktonic system. Comput. Math. Appl. **75**(12), 4490–4504 (2018)
45. Pang, G., Chen, L.: Periodic solution of the system with impulsive state feedback control. Nonlinear Dyn. **78**(1), 743–753 (2014)
46. Lv, W., Wang, F., Li, Y.: Adaptive finite-time tracking control for nonlinear systems with unmodeled dynamics using neural networks. Adv. Differ. Equ. **2018**(1), 159 (2018)
47. Tang, S., Chen, L.: Global attractivity in a food-limited population model with impulsive effects. J. Math. Anal. Appl. **292**(1), 211–221 (2004)
48. Zhuo, X.: Global attractability and permanence for a new stage-structured delay impulsive ecosystem. J. Appl. Anal. Comput. **8**(2), 457–470 (2018)
49. Tian, Y., Zhang, T., Sun, K.: Dynamics analysis of a pest management prey–predator model by means of interval state monitoring and control. Nonlinear Anal. Hybrid Syst. **23**, 122–141 (2017)
50. Ling, Z., Zhang, L., Zhu, M., Malay, B.: Dynamical behaviour of a generalist predator–prey model with free boundary. Bound. Value Probl. **2017**(1), 139 (2017)
51. Zeng, G.Z., Chen, L.S., Chen, J.F.: Persistence and periodic orbits for two-species nonautonomous diffusion Lotka–Volterra models. Math. Comput. Model. **20**(12), 69–80 (1994)
52. Nie, L., Teng, Z., Hu, L.: The dynamics of a chemostat model with state dependent impulsive effects. Int. J. Bifurc. Chaos **21**(05), 1311–1322 (2011)